BNL-225280-2024-JAAM

GRP-COPD-12

Red-Colored Circularly Polarized Luminescence from a Benzo-Fused BODIPY-BINOL Complex

M. Tsuji, T. Mani

To be published in "The Journal of Physical Chemistry B"

November 2023

Chemistry Department

Brookhaven National Laboratory

U.S. Department of Energy

USDOE Office of Science (SC), Basic Energy Sciences (BES)

DISCLAIMER

Red Colored Circularly Polarized Luminescence from a Benzo-fused BODIPY-BINOL Complex

Miu Tsuji,[1] Sara Abuhadba,[2] Angela Chen,[1] Mio Ito,[3] Amrita Makhijani,[1] Yutaka Kuwahara,[3,4] Tatiana Esipova,[2] and Tomoyasu Mani[1,5]*

[1] Department of Chemistry, University of Connecticut, Storrs CT 06269, United States

[2] Department of Chemistry and Biochemistry, Loyola University Chicago, Chicago, Illinois 60660, United States

[3] Department of Applied Chemistry and Biochemistry, Kumamoto University, 2-39-1 Kurokami, Chuo-ku, Kumamoto 860-8555, Japan.

[4] International Research Organization for Advanced Science and Technology (IROAST), Kumamoto University, 2-39-1 Kurokami, Chuo-ku, Kumamoto 860-8555, Japan

[5] Chemistry Division, Brookhaven National Laboratory, Upton NY 11973, United States

ABSTRACT: Red emission with sharp bandwidth and high quantum yield are desired characteristics for organic chromophores in optoelectronic, spintronic, and biomedical applications. Here, we observe circularly polarized luminescence (CPL) with these characteristics from a benzo-fused BODIPY-BINOL complex (**1**). Using time-resolved optical spectroscopy, electrochemistry, and density functional theory calculations, we showed that the emissive excited state of **1** does not have a charge-transfer character, unlike the regular BODIPY counterpart (**2**). The rigidity and the lack of charge-transfer character make this class of molecules an appealing platform for CPL-active molecules in the red spectral region with ample room for improvement in the dissymmetry factor and brightness.

1. Introduction

Circularly polarized luminescence (CPL) is an emerging field of research with the potential for material and biological applications.[1-3] CPL emits light with a distinct handedness, either left-handed or right-handed circular polarization. This unique property provides exciting possibilities for various fields, including optoelectronics,[4-6] security devices,[7] chiral sensing,[8] and quantum information technologies.[9]

The CPL is quantified by the dissymmetry factor $g_{\mathrm{lum}} = 2\frac{I_{\mathrm{L}}-I_{\mathrm{R}}}{I_{\mathrm{L}}+I_{\mathrm{R}}}$ where I_{L} and I_{R} are the left and right CP components of the emission.[10] Adopting the brightness of chromophores (B) that takes into account the extinction coefficient (ε_λ) measured at the excitation wavelength and the emission quantum yield (Φ),[11] one can define a brightness for CPL (B_{CPL})[12] as

$$B_{\mathrm{CPL}} = \varepsilon_\lambda \times \Phi \times \frac{|g_{\mathrm{lum}}|}{2} = B \times \frac{|g_{\mathrm{lum}}|}{2} \qquad (1)$$

where B_{CPL} is expressed in terms of $\mathrm{M^{-1}cm^{-1}}$. Replacing ε_λ by the efficiency of light absorption, we can also define a circularly polarization luminosity (Λ_{CPL}, which takes values from 0 to 1).[13] We can obtain higher B_{CPL} by increasing ε_λ, Φ, and g_{lum} individually. While organic chromophores usually have lower g_{lum}, they tend to have higher ε_λ and Φ, compared to metal complexes that can exhibit higher g_{lum}. Another consideration for applications is bandwidth. Narrow bandwidth is preferred for high purity (e.g., organic light-emitting diodes) and selectivity (e.g., multiplexed imaging).[14] While π-conjugated organic chromophores tend to have significantly higher ε_λ (a couple of orders magnitude higher), their bandwidth is generally broader compared to metal-centered emission (e.g., lanthanides).[15] Therefore, there is a strong push to develop narrowband organic emitters,[16] and with such molecules, one can realize the full potential of CPL-active organic chromophores.

Boron dipyrromethene (BODIPY or BD) dyes are a class of molecules that can be synthetically modified to emit CPL. Some advantages of BODIPY dyes include large ε_λ (~ 5 – 10 × 10^4 $\mathrm{M^{-1}cm^{-1}}$) and high Φ. Their thermal and photochemical stabilities also make them robust and reliable for materials and biological applications. The tunability of the optical and electrochemical properties of BODIPY molecules is remarkable,[17-18] allowing for a wide range of modifications to tailor their optical properties to specific applications. While these properties make BODIPY an attractive and versatile class of molecules for CPL, the number of BODIPY-based CPL emitting chromophores is still not large, [12] compared to other types of organic molecules (e.g., helicenes[19]), and many of them require chiral column chromatography to isolate enantiomers.[20-25] Some reported compounds with B_{CPL} are shown in **Table S1**.

One exception is BODIPY-BINOL complexes, where simple complexations attach an axially chiral 1,1'-binaphthyl unit to the BODIPY chromophore.[26-29] This class of molecules can exhibit electronic circular dichroism (ECD) and CPL despite the main chromophore being achiral. The emissive states are largely of charge-transfer (CT) character[26-27] (see below for details), likely making them CPL active.

Here, we disclosed a benzo-fused BODIPY-BINOL derivative (**1**, **Chart1**), where we observed a red-wavelength CPL with B_{CPL} = 25 $\mathrm{M^{-1}cm^{-1}}$. In a similar manner to regular

BODIPYs, we can render chirality to a benzo-fused BODIPY by complexation with BINOL.

Chart 1. Structures of the Molecules Studied.

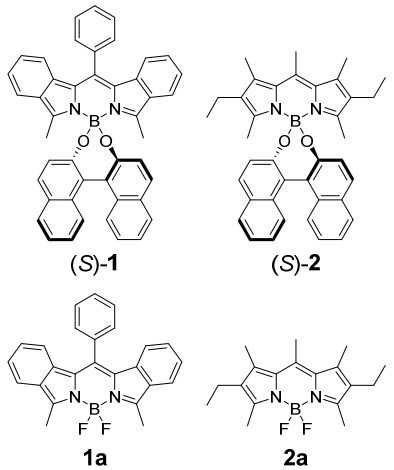

Unlike the regular BODIPY counterparts, our experimental and computational results show that the emissive excited states do not have a CT character and are instead local to BODIPY, maintaining a rather sharp-emission bandwidth, measured as the full-width half-maximum (fwhm)~ 25 nm of the 0-0 vibronic transition, and very high Φ (~1.0). Because of the relative ease of synthesis of benzo-fused BODIPYs[30-32] and as we don't need to use chiral HPLC for isolation, this family of molecules can be a unique platform for red-emitting CPL-active molecules. Highly emissive CPL-active molecules in the red and near-infrared regions are particularly promising for biological sensing and imaging[33-34] as well as quantum information technologies.[9]

2. Methods

2.1. General

All reagents and solvents were sourced from standard commercial chemical supply companies, unless noted otherwise. Silica gel (pore size 60 Å, 230–400 mesh, SiliCycle Inc.) was used in manual flash column chromatography. The ^{1}H and ^{13}C NMR spectra were recorded via a Bruker Avance III spectrometer, operating at 400.14 and 100.62 MHz, respectively. The mass spectra were obtained via QStar Elite (AB Sciex) conducted at the Laboratory of Mass Spectrometry and Omics Analysis of the University of Connecticut Department of Chemistry. UV–vis absorption spectra were recorded by a Cary 60 Scan UV–vis spectrophotometer (Agilent).

2.2. Optical Spectroscopy

A FLS1000 photoluminescence spectrometer (Edinburgh Instruments) was used to record the steady-state and time-resolved emission. Fluorescence lifetime measurements were performed using a TCSPC system of the FLS1000 equipped with a TCSPC/MCS/counter module (TCC2), a Hamamatsu H10720-01P, and a pulsed diode laser (EPL-405 or EPL-510) as the excitation source that provided 405 or 506 nm excitation with a pulse duration of 55 or 85 ps. Using the FLS1000 equipped with an integrating sphere, absolute measurements were conducted to obtain quantum yields of fluorescence (Φ). Circularly polarized luminescence measurements were conducted with a CPL accessory of the FLS1000 spectrometer. The concentration of the solutions for CPL measurements was kept < 0.5 μM. All the photophysical characterizations were conducted at room temperature (20 °C).

Femtosecond transient absorption (fsTA) measurements were conducted by using a system based on the HELIOS FIRE (Ultrafast Systems) coupled with a femtosecond laser system (Coherent). The details were reported elsewhere.[35]

2.3. Electrochemistry

Cyclic voltammetry (CV) measurements were conducted on all three samples based on a 600E Electrochemical Analyzer/Workstation (CH Instruments). This system was equipped with a standard three-electrode cell comprised of a pseudo-Ag reference electrode, a Pt wire counter electrode, and a 3 mm glassy carbon-disk working electrode in acetonitrile (MeCN) solution of 0.1 M tetrabutylammonium hexafluorophosphate ($TBA^{+}PF_{6}^{-}$). Datasets were processed and analyzed with the software CHI600e (CH Instruments). Potentials measured are referenced vs. $Fc^{+/0}$; ferrocene was introduced before measurements.

2.4. Computational Chemistry

Computations were carried out with Gaussian16.[36] The geometries were optimized with B3LYP[37-38] functional in density functional theory (DFT) calculations. The 6-31+G(d) was used for the geometry optimization and TDDFT single-point energy calculations. The polarizable continuum model (PCM)[39-41] was used as implemented in Gaussian. The excited state analysis was performed by using the Multiwfn software.[42].

2.5. Synthesis

1a (Chart 1) was synthesized by using the method developed by N. Ono,[32] and (*R*)- and (*S*)-**2** were synthesized from the precursor BODIPY **2a** (PM567, Chart 1) as described.[26] **2a** was purchased from Sigma Aldrich.

1. A mixture of **1a** (90 mg, 0.23 mmol) and aluminum chloride (75 mg, 0.56 mmol) in anhydrous CH_2Cl_2 (6 ml) was stirred for 10 min at room temperature under a nitrogen atmosphere. A solution of the enantiopure (*S*)-BINOL or (*R*)-BINOL (300 mg, 1.0 mmol) in anhydrous MeCN (15 ml) was added dropwise. The resulting mixture was stirred for 2 hours. Then, deionized water (2 ml) was added, and the mixture was stirred for a further 30 min. Then, the reaction mixture was extracted with CH_2Cl_2, dried over anhydrous $MgSO_4$, filtered, and evaporated. The crude compound was purified by silica gel chromatography (CH_2Cl_2/hexanes) to afford the desired product as a dark blue solid.

(*R*)-**1** (70 mg, yield 47%). ^{1}H NMR (400 MHz, CD_2Cl_2) δ 7.89 (d, 2H), 7.80 (d, 2H), 7.75 – 7.66 (m, 3H), 7.65 – 7.58 (m, 2H), 7.44 – 7.34 (m, 4H), 7.31 – 7.25 (m, 2H), 7.24 – 7.15 (m, 4H), 7.05 – 6.93 (m, 4H), 6.16 (d, 2H), 2.07 (s, 6H). 13C NMR (101 MHz, CD_2Cl_2) δ 154.28, 151.47, 135.76, 134.87, 133.86, 133.75, 130.80, 130.21, 129.58, 129.45, 129.22, 129.17, 128.40, 128.05, 126.96, 125.47, 125.39, 123.56, 123.45, 121.88, 121.47, 121.13, 53.95, 53.68, 53.41, 53.14, 52.87, 29.69, 13.12. HRMS (ES+) m/z: $[M]^{+}$ calcd 642.2481, found 642.2476.

(*S*)-**1**: (17 mg, yield 12 %). HRMS (ES+) m/z: $[M]^{+}$ calcd 642.2481, found 642.2472.

Table 1. Photophysical Characteristics[a]

	λ_{abs} (nm)	ε ($M^{-1}cm^{-1}$)	λ_{em} (nm)	Φ	fwhm (cm^{-1})[b]	fwhm (nm)[b]	τ_{fl} (ns)	k_{nr} (s^{-1})	$\lvert g_{lum}\rvert$[c]	B_{CPL} ($M^{-1}cm^{-1}$)[c]
1	606	103000	619	0.97	653	25	6.2	4.2×10^6	5.1×10^{-4}	25
1a	606	123000	615	0.97	608	23	5.7	5.3×10^6	NA	NA
2	525	53000	558	0.44	2322	72	4.5	1.3×10^8	6.2×10^{-4}	7
2a	523	58000	540	0.90	1753	51	6.0	1.7×10^7	NA	NA

[a] Reported in chloroform. [b] fwhm of the 0-0 vibronic transition. [c] Reported as the average of (*R*) and (*S*) enantiomers.

3. Results

The absorption and emission spectra of (*S*)-**1** and (*S*)-**2** in chloroform are shown in **Figure 1**, and some basic photophysical characteristics are reported in **Table 1**.

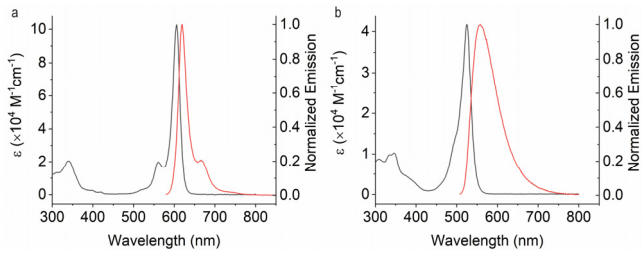

Figure 1. Normalized absorption and emission spectra of (a) (*S*)-**1** and (b) (*S*)-**2** in chloroform.

The linewidth of **1**, measured as fwhm, is ~3.5 times smaller than **2**. The extinction coefficient of **1** is about two times higher than that of **2**, and **1** maintains a very high $\Phi = 0.97$ and, therefore, a low nonradiative decay rate ($k_{nr} \sim 4.2 \times 10^6$ s^{-1}) even with the complexation with BINOL. Overall, **1** retains the key photophysical characteristics of the precursor **1a**[32] even after complexation, while we see the changes between **2** and **2a**. The radiative decays (k_r) of all four compounds are 1-1.5 × 10^8 s^{-1} in chloroform.

ECD and CPL of (*S*)- and (*R*)-**1** in chloroform are shown in **Figure 2**, along with those of (*S*)- and (*R*)-**2**. We also measured the CPL of (*R*)-**1** and (*R*)-**2** in toluene and MeCN, which are reported in **Figure S1**. Please note that Sánchez-Carnerero et al. reported the sign change between ECD and CPL for (*S*)- and (*R*)-**2**,[26] but we did not observe such a change in our study. While the previous computational study[43] suggested that the different conformations of flexible ethyl groups at the β position may result in the opposite sign of the CPL, it is unclear if one can have significantly different populations of one conformer or the other under similar conditions (in solution at room temperature). Nevertheless, our results show that the CPL of **2** exhibits the same sign as ECD.

We also recorded the emission spectra and lifetimes of **1** and **2** in toluene (nonpolar solvent) and MeCN (polar solvent). While the emission properties of **1** are relatively insensitive to solvent polarity, the lifetime of **2** becomes shorter in MeCN. The decay is biphasic, with short and long lifetimes being τ_{fl} = 0.56 and 5.8 ns, respectively (**Figure S2**). This reduction in lifetime is accompanied by a significant decrease in quantum yield (Φ = 0.06 in MeCN), suggesting enhanced nonradiative decay.

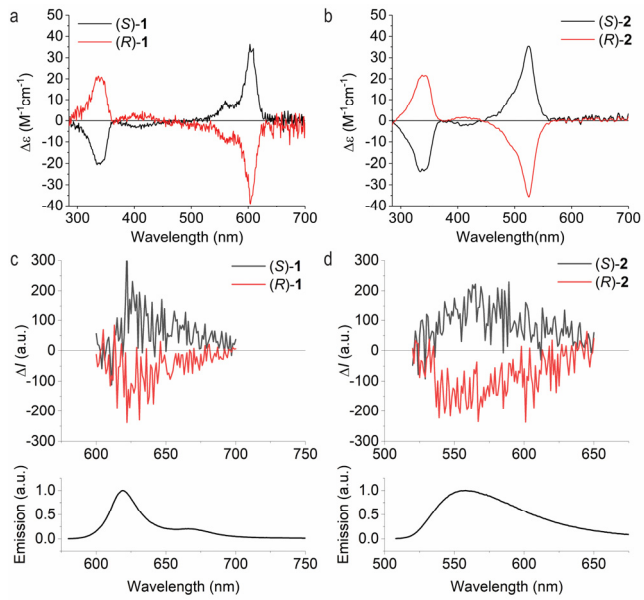

Figure 2. ECD spectra of (a) **1** and (b) **2** in chloroform. CPL and emission spectra of (c) **1** and (d) **2** in chloroform.

To clarify the photophysical pathways, we performed the fsTA spectroscopy. The decay-associated spectra (DAS) spectra in chloroform are shown in **Figure 3**.

The faster component of DAS is likely associated with vibrational cooling[44]; they are about two times faster in **2** and **2a** than in **1** and **1a**. The excited state dynamics of **1** and **1a** are similar without apparent observable differences within the UV-visible spectral region examined (**Figure 3a-b**). In contrast, we observed some differences between **2** and **2a** (**Figure 3c-d**). The most noticeable difference is the emissive peak in the 520-600 nm region, which corresponds to the stimulated CT emission, and roughly to the absorption of $BD^{\bullet-}$ (~ 560 nm).[35] We also observed a new broad peak around 400 nm from **2** in MeCN (**Figure 3e**). We did not observe any long-lived species (i.e., triplet excited states). The new species observed in the fsTA measurements is likely due to the movement of charges upon photoexcitation.

We determined the reduction potentials by CV in MeCN to elucidate the energetics of possible photogenerated species. The voltammograms of **1** and **2** are shown in **Figure S3**. The reduction potentials are reported in **Table 2**.

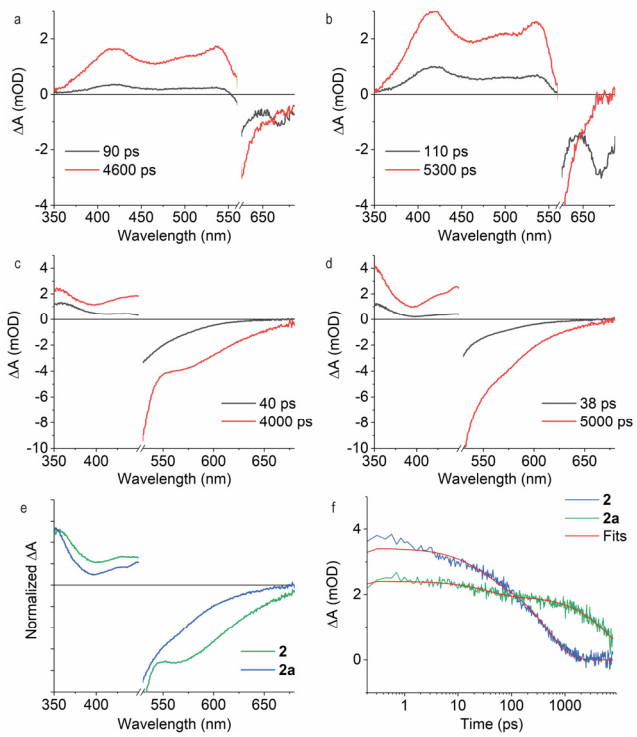

Figure 3. fsTA measurements elucidate the difference between **1** and **2** upon photoexcitation. DAS of (a) (*S*)-**1** and (b) **1a** in chloroform (λ_{ex} = 600 nm). DAS of (c) (*S*)-**2** and (d) **2a** in chloroform (λ_{ex} = 500 nm). The numbers in the legend correspond to the lifetimes. (e) The normalized DAS of the longer lifetime of (*S*)-**2** and **2a** in MeCN (λ_{ex} = 500 nm). (f) Decay kinetics at 400 nm for (*S*)-**2** and **2a** in MeCN (λ_{ex} = 500 nm). The fits are fitted curves to the double exponential decay with the instrument response function.

Table 2. Electrochemical Properties[a]

	$E_{ox}^{BD,2}$	E_{ox}^{BINOL}	E_{ox}^{BD}	E_{red}^{BD}	$E_{red}^{BD,2}$
1	1.21	0.97[b]	0.26	-1.60	-2.27
1a	1.17	--	0.32	-1.55	-2.27
2	ND[c]	0.89[b]	0.57	-1.73	-2.70
2a	ND[c]	--	0.59	-1.72	-2.68

[a] Reported V vs. $Fc^{+/0}$. Measured in MeCN with 0.1 M $TBA^+PF_6^-$. The errors are usually 10-20 mV. [b] Irreversible. [c] ND = Not determined.

1a showed the reduction potentials of the dication ($E_{ox}^{BD,2}$) and radical cation (E_{ox}^{BD}) as well as those of the neutral (E_{red}^{BD}) and the radical anion ($E_{red}^{BD,2}$) of a benzo-fused BODIPY. E_{ox}^{BD} and E_{red}^{BD} agree with those reported earlier.[32] In addition, the measurement of **1** revealed the additional peak that corresponds to the reduction potential of the radical cation of BINOL (E_{ox}^{BINOL}) at 0.97 V vs. $Fc^{+/0}$ that is ~0.7 V larger than E_{ox}^{BD}. This is a clear contrast to **2,** where E_{ox}^{BINOL} is only 0.3 V above E_{ox}^{BD}. Note that the electrochemical oxidation of the BINOL moiety in **1** and **2** under the examined condition was irreversible.

4. Discussions

ECD and CPL data show that **1** is chiroptical active, making **1** a CPL-active chromophore with intense absorption/emission in the red spectral region (**Table 1**). We observed CPL from **1** and **2** in the three solvents of different polarity. The 0-1 vibronic band of **1** appears to be more CPL active, but a more rigorous study is likely necessary for clarifications. Our discussion below is focused on the differences and similarities between a benzo-fused BODIPY **1** and a regular BODIPY **2**. Based on the available data, we present the energy diagrams of **1** and **2** in **Figure 4** and use them for the discussions below.

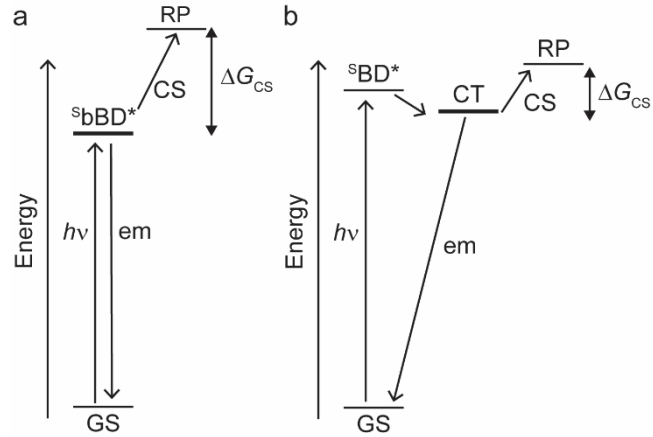

Figure 4. Energy diagrams of (a) **1** and (b) **2**. Please note that the energy is not in scale, and triplet excited states are not shown for brevity. bBD = benzo-fused BODIPY and BD = BODIPY.

The photoexcitation of **2** leads to the formation of the charge-transfer (CT) state in which charges are not fully dissociated ($BD^{\delta-}$-$BINOL^{\delta+}$). Computations support experimental data. TDDFT calculations of **2** show that the first and second singlet excited states have a CT character with positive charges primarily on BINOL (**Figure 5**). The distance between electron and hole (r_{eh}) is only 2.8 Å. The molecular orbital contribution of the first excited state revealed that HOMO (61%) and HOMO-1 (39%) contribute to the hole of the first excited state where both HOMO and HOMO-1 are delocalized over BODIPY and BINOL (**Figure S4**), suggesting that it is not a complete charge-separated state. The contribution of HOMO and HOMO-1 is reversed for the second excited state (**Table S2**). The complete charge-separated state or RP ($BD^{\bullet-}$-$BINOL^{\bullet+}$) is energetically higher in all the solvents. Computationally, we can identify it as the third excited state with ~0.6 eV higher energy than the first (**Table S2**). The analysis showed that HOMO-2 (98%) and LUMO (99%) contribute to hole and electron distributions, respectively, where HOMO-2 is localized to BODIPY (**Figure S4**).

Yet, the stabilization of charges in a polar solvent, MeCN, makes the RP energetically closer to the emissive CT state. We experimentally estimated the Gibbs energy difference of complete charge separation (from CT state to RP) in MeCN based on

$$\Delta G_{CS} = e(E_{ox}^{BINOL} - E_{red}^{BD}) - \frac{e^2}{4\pi\varepsilon_0\varepsilon_S r_{eh}} - E_{CT} \qquad (2)$$

where E_{CT} is the energy of CT state, ε_0 and ε_S are the vacuum permittivity and solvent dielectric constant of MeCN, respectively, and r_{eh} is the distance between electron (in BD) and hole (in BINOL). Note that we measured the reduction potential in MeCN. With E_{CT} = 2.34 eV and r_{eh} = 6 Å, the estimated ΔG_{CS} is + 0.2 eV (CT state to RP). While it

is uphill, ΔG_{CS} in MeCN becomes relatively smaller than in more nonpolar solvents. This makes the CT state in MeCN have more of an RP character, which results in the observed reduction of fluorescence lifetime (**Figure S2** for emission and **Figure 3f** for excited states' dynamics).

In contrast, we did not observe clear CT or RP states (bBD$^{\bullet}$-BINOL$^{\bullet+}$) of **1** upon photoexcitation in all solvents tested. This is also supported by electrochemical measurements as well as computational chemistry. DFT calculations show that the first excited state of **1** is local to a benzo-fused BODIPY (both electron and hole are localized to benzo-fused BD) while the second is the RP state (**Figure 5**, **Table S3**).

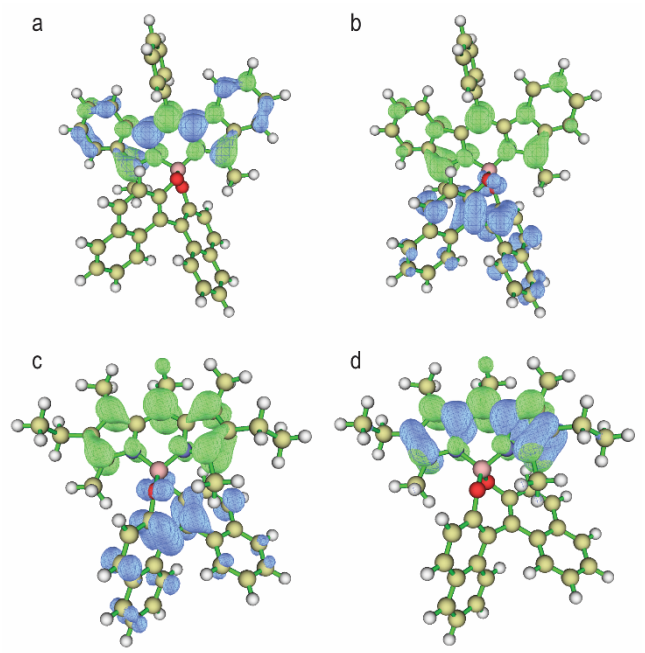

Figure 5. Electron (green) and hole (blue) distribution for the singlet excited states of (a) the first and (b) the second excited state of (*R*)-**1**, and (c) the first and (d) the second excited state of (*R*)-**2**. The calculations were performed at the level of B3LYP/6-31G+(d)/PCM (chloroform).

A lower reduction potential of the BODIPY radical cation makes the energy gap between E_{ox}^{BD} and E_{ox}^{BINOL} significant enough to prevent a hole delocalization. We can calculate ΔG_{CS} for the transition from S1 to RP in a similar manner to eq. 2; E_{CT} is replaced by E_{S1}. The lower singlet excited state energy of **1** (E_{S1} = 2.07 eV), compared to **2**, makes $\Delta G_{CS} \sim +0.43$ eV, using r_{eh} = 5.2 Å (**Table S3**). The value is significantly uphill to have the mixing of S1 with the RP,[45-47] even in a polar solvent.

The presented data showed a lesser extent of electronic communication in **1** than **2** between BODIPY and BINOL. Nonetheless, we could observe ECD and CPL from **1** (**Figure 2**), suggesting the structural perturbation on the BODIPY core forced by the complexation of BINOL is strong enough for induction of chiroptical activity of BODIPY.

5. Conclusions

We present a benzo-fused BODIPY-BINOL molecule (**1**) that exhibits strong CPL (B_{CPL} = 25 M^{-1}cm^{-1}) with narrowband emission (fwhm ~25 nm or ~650 cm^{-1}). This is among the brightest BODIPY-based CPL active chromophores without the need of chiral HPLC (**Figure S5** and **Table S1**). Rigid structures and a lack of CT character in the excited state are crucial for developing organic chromophores with narrowband emission that is desirable for optoelectronic and biological applications.[16] A benzo-fused BODIPY has the required rigidity imparted by a fusion of benzene rings. We also showed that **1** does not undergo a photoinduced charge shift/separation process, making it possible for **1** to preserve the desired nature of its precursor **1a**. BODIPY and BINOL are mostly electronically decoupled, and the emission of **1** has no CT character. In contrast, we demonstrated that the regular BODIPY counterpart (**2**) undergoes such charge delocalization/separation process upon photoexcitation, as previously speculated.[27] In summary, structural perturbation is likely the primary source of chiroptical activity in **1** and possibly other BODIPY-BINOL complexes. Our study suggests that we can further improve the performance of CPL in the red spectra region with the current platform by appropriate electronic controls by functionalizing a benzo-fused BODIPY core and BINOLs while maintaining the rigidity and appropriate redox properties that warrant high Φ.

ASSOCIATED CONTENT

Figure S1-5, Table S1-3, Coordinates used for computational chemistry, additional references, and NMR data.
This material is available free of charge via the Internet at http://pubs.acs.org.

AUTHOR INFORMATION

Corresponding Author

* tomoyasu.mani@uconn.edu

Author Contributions

All authors have given approval to the final version of the manuscript.

ACKNOWLEDGMENT

The authors acknowledge funding by the National Science Foundation under Grant No. 2144787, an NSF CAREER Award (T.M.), and No. 2247661 (T.E.), 2247662 (T.M.). The work is, in part, supported through IROAST (Y.K. and T.M.). The computational studies were performed at the cluster located in the Chemistry Division of the Brookhaven National Laboratory through work funded by LDRD 23-030 (T.M.).

REFERENCES

1. MacKenzie, L. E.; Pal, R. Circularly polarized lanthanide luminescence for advanced security inks. *Nat. Rev. Chem.* **2021,** *5*, 109-124, DOI: 10.1038/s41570-020-00235-4
2. Ma, J.-L.; Peng, Q.; Zhao, C.-H. Circularly Polarized Luminescence Switching in Small Organic Molecules. *Chem. Eur. J.* **2019,** *25*, 15441-15454, DOI: 10.1002/chem.201903252
3. Longhi, G.; Castiglioni, E.; Koshoubu, J.; Mazzeo, G.; Abbate, S. Circularly Polarized Luminescence: A Review of Experimental and Theoretical Aspects. *Chirality* **2016,** *28*, 696-707, DOI: 10.1002/chir.22647
4. Yoon, G.; Lee, D.; Nam, K. T.; Rho, J. "Crypto-Display" in Dual-Mode Metasurfaces by Simultaneous Control of Phase and Spectral Responses. *Acs Nano* **2018,** *12*, 6421-6428, DOI: 10.1021/acsnano.8b01344

5. Zhang, D.-W.; Li, M.; Chen, C.-F. Recent advances in circularly polarized electroluminescence based on organic light-emitting diodes. *Chem. Soc. Rev.* **2020,** *49*, 1331-1343, DOI: 10.1039/C9CS00680J

6. Dhbaibi, K.; Abella, L.; Meunier-Della-Gatta, S.; Roisnel, T.; Vanthuyne, N.; Jamoussi, B.; Pieters, G.; Racine, B.; Quesnel, E.; Autschbach, J., et al. Achieving high circularly polarized luminescence with push–pull helicenic systems: from rationalized design to top-emission CP-OLED applications. *Chem. Sci.* **2021,** *12*, 5522-5533, DOI: 10.1039/D0SC06895K

7. Kitagawa, Y.; Wada, S.; Islam, M. D. J.; Saita, K.; Gon, M.; Fushimi, K.; Tanaka, K.; Maeda, S.; Hasegawa, Y. Chiral lanthanide lumino-glass for a circularly polarized light security device. *Commun. Chem.* **2020,** *3*, 119, DOI: 10.1038/s42004-020-00366-1

8. Carr, R.; Evans, N. H.; Parker, D. Lanthanide complexes as chiral probes exploiting circularly polarized luminescence. *Chem. Soc. Rev.* **2012,** *41*, 7673-7686, DOI: 10.1039/C2CS35242G

9. Lodahl, P.; Mahmoodian, S.; Stobbe, S.; Rauschenbeutel, A.; Schneeweiss, P.; Volz, J.; Pichler, H.; Zoller, P. Chiral quantum optics. *Nature* **2017,** *541*, 473-480, DOI: 10.1038/nature21037

10. Riehl, J. P.; Richardson, F. S. Circularly polarized luminescence spectroscopy. *Chem. Rev.* **1986,** *86*, 1-16, DOI: 10.1021/cr00071a001

11. Wong, K.-L.; Bünzli, J.-C. G.; Tanner, P. A. Quantum yield and brightness. *J. Lumin.* **2020,** *224*, 117256, DOI: 10.1016/j.jlumin.2020.117256

12. Arrico, L.; Di Bari, L.; Zinna, F. Quantifying the Overall Efficiency of Circularly Polarized Emitters. *Chem. Eur. J.* **2021,** *27*, 2920-2934, DOI: 10.1002/chem.202002791

13. Nagata, Y.; Mori, T. Irreverent Nature of Dissymmetry Factor and Quantum Yield in Circularly Polarized Luminescence of Small Organic Molecules. *Front. Chem.* **2020,** *8*, 448, DOI: 10.3389/fchem.2020.00448

14. Zhou, X.; Zhao, L.; Zhang, K.; Yang, C.; Li, S.; Kang, X.; Li, G.; Wang, Q.; Ji, H.; Wu, M., et al. Ultrabright AIEdots with tunable narrow emission for multiplexed fluorescence imaging. *Chem. Sci.* **2023,** *14*, 113-120, DOI: 10.1039/D2SC04862K

15. Zinna, F.; Di Bari, L. Lanthanide Circularly Polarized Luminescence: Bases and Applications. *Chirality* **2015,** *27*, 1-13, DOI: 10.1002/chir.22382

16. Ha, J. M.; Hur, S. H.; Pathak, A.; Jeong, J.-E.; Woo, H. Y. Recent advances in organic luminescent materials with narrowband emission. *NPG Asia Materials* **2021,** *13*, 53, DOI: 10.1038/s41427-021-00318-8

17. Ziessel, R.; Ulrich, G.; Harriman, A. The chemistry of Bodipy: a new El Dorado for fluorescence tools. *New. J. Chem.* **2007,** *31*, 496-501, DOI: 10.1039/B617972j

18. Loudet, A.; Burgess, K. BODIPY dyes and their derivatives: Syntheses and spectroscopic properties. *Chem. Rev.* **2007,** *107*, 4891-4932, DOI: 10.1021/Cr078381n

19. Mori, T. Chiroptical Properties of Symmetric Double, Triple, and Multiple Helicenes. *Chem. Rev.* **2021,** *121*, 2373-2412, DOI: 10.1021/acs.chemrev.0c01017

20. Saikawa, M.; Nakamura, T.; Uchida, J.; Yamamura, M.; Nabeshima, T. Synthesis of figure-of-eight helical bisBODIPY macrocycles and their chiroptical properties. *Chem. Commun.* **2016,** *52*, 10727-10730, DOI: 10.1039/C6CC05439K

21. Alnoman, R. B.; Rihn, S.; O'Connor, D. C.; Black, F. A.; Costello, B.; Waddell, P. G.; Clegg, W.; Peacock, R. D.; Herrebout, W.; Knight, J. G., et al. Circularly Polarized Luminescence from Helically Chiral N,N,O,O-Boron-Chelated Dipyrromethenes. *Chem. Eur. J.* **2016,** *22*, 93-96, DOI: 10.1002/chem.201504484

22. Zinna, F.; Bruhn, T.; Guido, C. A.; Ahrens, J.; Bröring, M.; Di Bari, L.; Pescitelli, G. Circularly Polarized Luminescence from Axially Chiral BODIPY DYEmers: An Experimental and Computational Study. *Chem. Eur. J.* **2016,** *22*, 16089-16098, DOI: 10.1002/chem.201602684

23. Clarke, R.; Ho, K. L.; Alsimaree, A. A.; Woodford, O. J.; Waddell, P. G.; Bogaerts, J.; Herrebout, W.; Knight, J. G.; Pal, R.; Penfold, T. J., et al. Circularly Polarised Luminescence from Helically Chiral "Confused" N,N,O,C-Boron-Chelated Dipyrromethenes (BODIPYs). *ChemPhotoChem* **2017,** *1*, 513-517, DOI: 10.1002/cptc.201700106

24. Maeda, C.; Nagahata, K.; Shirakawa, T.; Ema, T. Azahelicene-Fused BODIPY Analogues Showing Circularly Polarized Luminescence. *Angew. Chem. Int. Edit.* **2020,** *59*, 7813-7817, DOI: 10.1002/anie.202001186

25. Wang, L.-Y.; Liu, Z.-F.; Teng, K.-X.; Niu, L.-Y.; Yang, Q.-Z. Circularly polarized luminescence from helical N,O-boron-chelated dipyrromethene (BODIPY) derivatives. *Chem. Commun.* **2022,** *58*, 3807-3810, DOI: 10.1039/D1CC06051A

26. Sánchez-Carnerero, E. M.; Moreno, F.; Maroto, B. L.; Agarrabeitia, A. R.; Ortiz, M. J.; Vo, B. G.; Muller, G.; Moya, S. d. l. Circularly Polarized Luminescence by Visible-Light Absorption in a Chiral O-BODIPY Dye: Unprecedented Design of CPL Organic Molecules from Achiral Chromophores. *J. Am. Chem. Soc.* **2014,** *136*, 3346-3349, DOI: 10.1021/ja412294s

27. Jiménez, J.; Moreno, F.; Maroto, B. L.; Cabreros, T. A.; Huy, A. S.; Muller, G.; Bañuelos, J.; de la Moya, S. Modulating ICT emission: a new strategy to manipulate the CPL sign in chiral emitters. *Chem. Commun.* **2019,** *55*, 1631-1634, DOI: 10.1039/C8CC09401B

28. Jiménez, J.; Díaz-Norambuena, C.; Serrano, S.; Ma, S. C.; Moreno, F.; Maroto, B. L.; Bañuelos, J.; Muller, G.; de la Moya, S. BINOLated aminostyryl BODIPYs: a workable organic molecular platform for NIR circularly polarized luminescence. *Chem. Commun.* **2021,** *57*, 5750-5753, DOI: 10.1039/D1CC01255J

29. Jiménez, J.; Moreno, F.; Arbeloa, T.; Cabreros, T. A.; Muller, G.; Bañuelos, J.; García-Moreno, I.; Maroto, B. L.; de la Moya, S. Isopinocampheyl-based C-BODIPYs: a model strategy to construct cost-effective boron-chelate emitters of circularly polarized light. *Org. Chem. Front.* **2021,** *8*, 4752-4757, DOI: 10.1039/D1QO00717C

30. Jean-Gérard, L.; Vasseur, W.; Scherninski, F.; Andrioletti, B. Recent advances in the synthesis of [a]-benzo-fused BODIPY fluorophores. *Chem. Commun.* **2018,** *54*, 12914-12929, DOI: 10.1039/C8CC06403B

31. Wada, M.; Ito, S.; Uno, H.; Murashima, T.; Ono, N.; Urano, T.; Urano, Y. Synthesis and optical properties of a new class of pyrromethene–BF2 complexes fused with rigid bicyclo rings and benzo derivatives. *Tetrahedron Lett.* **2001,** *42*, 6711-6713, DOI: 10.1016/S0040-4039(01)01299-0

32. Shen, Z.; Röhr, H.; Rurack, K.; Uno, H.; Spieles, M.; Schulz, B.; Reck, G.; Ono, N. Boron–Diindomethene (BDI) Dyes and Their Tetrahydrobicyclo Precursors—en Route to a New Class of Highly Emissive Fluorophores for the Red Spectral Range. *Chem. Eur. J.* **2004,** *10*, 4853-4871, DOI: 10.1002/chem.200400173

33. Tian, X.; Shoyama, K.; Mahlmeister, B.; Brust, F.; Stolte, M.; Würthner, F. Naphthalimide-Annulated [n]Helicenes: Red Circularly Polarized Light Emitters. *J. Am. Chem. Soc.* **2023,** *145*, 9886-9894, DOI: 10.1021/jacs.3c03441

34. Yuan, L.; Lin, W.; Zheng, K.; He, L.; Huang, W. Far-red to near infrared analyte-responsive fluorescent probes based on organic fluorophore platforms for fluorescence imaging. *Chem. Soc. Rev.* **2013,** *42*, 622-661, DOI: 10.1039/C2CS35313J

35. Buck, J. T.; Boudreau, A. M.; DeCarmine, A.; Wilson, R. W.; Hampsey, J.; Mani, T. Spin-Allowed Transitions Control the Formation of Triplet Excited States in Orthogonal Donor-Acceptor Dyads. *Chem* **2019,** *5*, 138-155, DOI: 10.1016/j.chempr.2018.10.001

36. Frisch, M. J.; Trucks, G. W.; Schlegel, H. B.; Scuseria, G. E.; Robb, M. A.; Cheeseman, J. R.; Scalmani, G.; Barone, V.; Petersson, G. A.; Nakatsuji, H., et al. *Gaussian 16 Rev. B.01*, Wallingford, CT, 2016.

37. Becke, A. D. Density-Functional Thermochemistry. III. The Role of Exact Exchange. *J. Chem. Phys.* **1993,** *98*, 5648-5652, DOI: Doi 10.1063/1.464913

38. Stephens, P. J.; Devlin, F. J.; Chabalowski, C. F.; Frisch, M. J. Ab-Initio Calculation of Vibrational Absorption and Circular-Dichroism Spectra Using Density-Functional Force-Fields. *J. Phys. Chem.* **1994,** *98*, 11623-11627, DOI: Doi 10.1021/J100096a001

39. Improta, R.; Scalmani, G.; Frisch, M. J.; Barone, V. Toward effective and reliable fluorescence energies in solution by a new state specific polarizable continuum model time dependent density functional theory approach. *J. Chem. Phys.* **2007,** *127*, 074504 074501-074509, DOI: Artn 074504
Doi 10.1063/1.2757168

40. Improta, R.; Barone, V.; Scalmani, G.; Frisch, M. J. A state-specific polarizable continuum model time dependent density functional theory method for excited state calculations in solution. *J. Chem. Phys.* **2006,** *125*, 054103 054101-054109, DOI: Artn 054103
Doi 10.1063/1.2222364

41. Tomasi, J.; Mennucci, B.; Cammi, R. Quantum Mechanical Continuum Solvation Models. *Chem. Rev.* **2005,** *105*, 2999-3094, DOI: 10.1021/cr9904009

42. Tian, L.; Feiwu, C. Multiwfn: A multifunctional wavefunction analyzer. *J. Comput. Chem.* **2012,** *33*, 580-592, DOI: doi:10.1002/jcc.22885

43. Yang, Q.; Fusè, M.; Bloino, J. Theoretical Investigation of the Circularly Polarized Luminescence of a Chiral Boron Dipyrromethene (BODIPY) Dye. *Front. Chem.* **2020,** *8*, 801, DOI: 10.3389/fchem.2020.00801

44. Rosspeintner, A.; Lang, B.; Vauthey, E. Ultrafast Photochemistry in Liquids. *Annu. Rev. Phys. Chem.* **2013,** *64*, 247-271, DOI: 10.1146/annurev-physchem-040412-110146

45. Murrell, J. N. Molecular Complexes and their Spectra. IX. The Relationship between the Stability of a Complex and the Intensity of its Charge-transfer Bands1. *J. Am. Chem. Soc.* **1959,** *81*, 5037-5043, DOI: 10.1021/ja01528a007

46. Bixon, M.; Jortner, J.; Verhoeven, J. W. Lifetimes for Radiative Charge Recombination in Donor-Acceptor Molecules. *J. Am. Chem. Soc.* **1994,** *116*, 7349-7355, DOI: 10.1021/ja00095a044

47. Gould, I. R.; Young, R. H.; Mueller, L. J.; Albrecht, A. C.; Farid, S. Electronic-Structures of Exciplexes and Excited Charge-Transfer Complexes. *J. Am. Chem. Soc.* **1994,** *116*, 8188-8199, DOI: Doi 10.1021/Ja00097a028

TOC Graphic

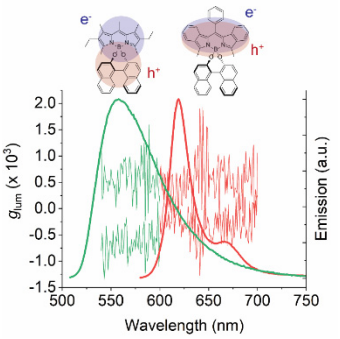
e⁻
h⁺
e⁻
h⁺
2.0
1.5
1.0
0.5
0.0
-0.5
-1.0
-1.5
g_{lum} (x 10^3)
500
550
600
650
700
750
Wavelength (nm)
Emission (a.u.)